

# Chapter 13

## Network Dynamics

Herbert M. Sauro

### Abstract

Probably one of the most characteristic features of a living system is its continual propensity to change as it juggles the demands of survival with the need to replicate. Internally these adjustments are manifest as changes in metabolite, protein, and gene activities. Such changes have become increasingly obvious to experimentalists, with the advent of high-throughput technologies. In this chapter we highlight some of the quantitative approaches used to rationalize the study of cellular dynamics. The chapter focuses attention on the analysis of quantitative models based on differential equations using biochemical control theory. Basic pathway motifs are discussed, including straight chain, branched, and cyclic systems. In addition, some of the properties conferred by positive and negative feedback loops are discussed, particularly in relation to bistability and oscillatory dynamics.

**Key words:** Motifs, control analysis, stability, dynamic models.

---

### 1. Introduction

Probably, one of the most characteristic features of a living system is its continual propensity to change even though it is also arguably the one characteristic that, as molecular biologists, we often ignore. Part of the reason for this neglect is the difficulty in making time-dependent quantitative measurements of proteins and other molecules although that is rapidly changing with advances in technology. The dynamics of cellular processes, and in particular cellular networks, is one of the defining attributes of the living state and deserves special attention.

Before proceeding to the main discussion, it is worth briefly listing the kinds of questions that can and have been answered by a quantitative approach (*See Table 13.1*). For example, the notion

**Table 13.1**  
**Some problems amenable to a quantitative approach**

<b>Problem</b>	<b>Representative solution</b>
Rate-limiting steps	Kacser and Burns (49)
Role of feedback and robustness	Savageau (77)
Analysis of cell-to-cell variation	Mettetal et al. (61)
Rationalization of network structure	Voit et al. (87)
Design of synthetic networks	Kaern and Weiss (51)
New principles of regulation	Altan-Bonnet and Germain (1)
New therapeutic approaches	Bakker et al. (5)
Origin of dominance and recessivity	Kacser and Burns (50)
Missing interactions	Ingolia (46)
Multistationary systems	Many Examples Exist (52)

of the rate-limiting step was originally a purely intuitive invention; once analyzed quantitatively, however, it was shown to be inconsistent with both logic and experimental evidence. There are many examples such as this where a quantitative analysis has overturned a long-held view of how cellular networks operate. In the long term, one of the aims of a quantitative approach is to uncover the general principles of cellular control and organization. In turn this will lead to new approaches to engineering organisms and the development of new therapeutics.

Although traditionally the discipline of molecular biology has had little need for the machinery of mathematics, the non-trivial nature of cellular networks and the need to quantify their dynamics have made mathematics a necessary addition to our arsenal. In this chapter we can sketch only some of the quantitative results and approaches that can be used to describe network dynamics. We will not cover topics such as flux balance, bifurcation analysis, or stochastic models, all important areas of study for systems biology. For the interested reader, much more detail can be had by consulting the reading list at the end of the chapter. Moreover, in this chapter we will not deal with the details of modeling specific systems because this topic is covered in other chapters.

### **1.1. Quantitative Approaches**

The most common formal approach to representing cellular networks has been to use a deterministic and continuous formalism, based invariably on ordinary differential equations (ODE). The reason for this is twofold, firstly ODEs have been shown in many cases to represent adequately the dynamics of real networks, and

secondly, there is a huge range of analytical results on the ODE-based models one can draw upon. Such analytical results are crucial to enabling a deeper understanding of the network under study.

An alternative approach to describing cellular networks is to use a discrete, stochastic approach, based usually on the solution of the master equation via the Gillespie method (27,28). This approach takes into account the fact that at the molecular level, species concentrations are whole numbers and change in discrete, integer amounts. In addition, changes in molecular amounts are assumed to be brought about by the inherent random nature of microscopic molecular collisions. In principle, many researchers view the stochastic approach to be a superior representation because it directly attempts to describe the molecular milieu of the cellular space. However, the approach has two severe limitations, the first is that the method does not scale, that is, when simulating large systems, particularly where the number of molecules is large ( $>200$ ), it is computationally very expensive. Secondly, there are few analytical results available to analyze stochastic models, which means that analysis is largely confined to numerical studies from which it is difficult to generalize. One of the great and exciting challenges for the future is to develop the stochastic approach to a point where it is as powerful a description as the continuous, deterministic approach. Without doubt, there is a growing body of work, such as studies on measuring gene expression in single cells, which depends very much on a stochastic representation. Unfortunately, the theory required to interpret and analyze stochastic models is still immature though rapidly changing (66, 78). The reader may consider the companion chapter by Resat et al. for the latest developments in stochastic dynamics.

In this chapter we will concentrate on some properties of network structures using a deterministic, continuous approach.

---

## 2. Stoichiometric Networks

The analysis of any biochemical network starts by considering the network's topology. This information is embodied in the stoichiometry matrix,  $N$  (**Note 1**). In the following description we will follow the standard formalism introduced by Reder (70). The columns of the stoichiometry matrix correspond to the distinct chemical reactions in the network, the rows to the molecular species, one row per species. Thus the intersection of a row and column in the matrix indicates whether a certain species takes part in a particular reaction or not, and, according to the sign of the

$$\begin{array}{c}
 \longleftarrow v_j \longrightarrow \\
 \uparrow \left[ \begin{array}{ccc} \alpha_{ij} & \dots & \dots \\ \vdots & & \\ \vdots & & \end{array} \right] \\
 \downarrow
 \end{array}$$

Fig. 13.1. Stoichiometry matrix:  $\mathbf{N}$ :  $m \times n$ , where  $\alpha_{ij}$  is the stoichiometric coefficient.  $S_i$  denotes the  $i$ th species, and  $v_j$  the  $j$ th reaction.

element, whether it is a reactant or product, and by the magnitude, the relative quantity of substance that takes part in that reaction. Stoichiometry thus concerns the relative mole amounts of chemical species that react in a particular reaction; it does not concern itself with the rate of reaction.

If a given network is composed of  $m$  molecular species involved in  $n$  reactions, then the stoichiometry matrix is an  $m \times n$  matrix. Only those molecular species that evolve through the dynamics of the system are included in this count. Any source and sink species needed to sustain a steady state (non-equilibrium in the thermodynamic sense) are set at a constant level and therefore do not have corresponding entries in the stoichiometry matrix (Fig. 13.1).

### 2.1. The System Equation

To fully characterize a system one also needs to consider the kinetics of the individual reactions as well as the network's topology. Modeling the reactions by differential equations, we arrive at a system equation that involves both the stoichiometry matrix and the rate vector, thus:

$$\frac{d\mathbf{S}}{dt} = \mathbf{N}\mathbf{v}, \quad [1]$$

where  $\mathbf{N}$  is the  $m \times n$  stoichiometry matrix and  $\mathbf{v}$  is the  $n$  dimensional rate vector, whose  $i$ th component gives the rate of reaction  $i$  as a function of the species concentrations.

### 2.2. Conservation Laws

In many models of real systems, there will be mass constraints on one or more sets of species. Such species are termed *conserved moieties* (71). A recent review of conservation analysis, which also highlights the history of stoichiometric analysis, can be found in (73). In this section only the main results will be given.

A typical example of a conserved moiety in a computational model is the conservation of adenine nucleotide, i.e., when the total amount of ATP, ADP, and AMP is constant during the evolution of the model. Other examples include NAD/NADH, phosphate, phosphorylated proteins forms, and so on. Figure 13.2 illustrates the simplest possible network that displays a conserved moiety; in this case the total mass,  $S_1 + S_2$ , is constant during the entire evolution of the network.

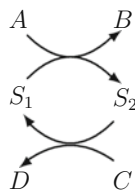


Fig. 13.2. Simple conserved cycle with the constraint,  $S_1 + S_2 = T$ .

The total amount of a particular moiety in a network is time-invariant and is determined solely by the initial conditions imposed on the system (**Note 2**).

Conserved moieties in the network reveal themselves as linear dependencies in the rows of the stoichiometry matrix (42, 14).

If we examine the system equations for the model depicted in **Fig. 13.2**, it is easy to see that the rate of appearance of  $S_1$  must equal the rate of disappearance of  $S_2$ , in other words  $dS_1/dt = -dS_2/dt$ . This identity is a direct result of the conservation of mass, namely that the sum  $S_1 + S_2$  is constant throughout the evolution of the system.

The stoichiometry matrix for the network depicted in **Fig. 13.2** has two rows  $[1, -1]$  and  $[-1, 1]$ . Since either row can be derived from the other by multiplication by  $-1$ , they are linearly dependent, and the rank of the matrix is 1. Whenever the network exhibits conserved moieties, there will be dependencies among the rows of  $N$ , and so the rank of  $N$  ( $\text{rank}(N)$ ) will be less than  $m$ , the number of rows of  $N$ . The rows of  $N$  can be rearranged so that the first  $\text{rank}(N)$  rows are linearly independent. The species which correspond to these rows can then be defined as the independent species ( $S_i$ ). The remaining  $m - \text{rank}(N)$  are called the dependent species ( $S_d$ ).

In the simple example shown in **Fig. 13.2**, there is one independent species,  $S_1$ , and one dependent species,  $S_2$  (or, alternatively,  $S_2$  is independent and  $S_1$  dependent).

Once the matrix  $N$  has been rearranged as described, we can partition it as

$$N = \begin{bmatrix} N_R \\ N_0 \end{bmatrix},$$

where the submatrix  $N_R$  is full rank, and each row of the submatrix  $N_0$  is a linear combination of the rows of  $N_R$ . Following Reder (69), we make the following construction. Since the rows of  $N_0$  are linear combinations of the rows of  $N_R$ , we can define a link-zero matrix  $L_0$  which satisfies  $N_0 = L_0 N_R$ . We can combine  $L_0$  with the identity matrix (of dimension  $\text{rank}(N)$ ) to form the link matrix  $L$  and hence we can write:

$$N = \begin{bmatrix} N_R \\ N_0 \end{bmatrix} = \begin{bmatrix} I \\ L_0 \end{bmatrix} N_R = L N_R.$$

By partitioning the stoichiometry matrix into dependent and independent sets, we also partition the system equation. The full system equation, which describes the dynamics of the network, is thus:

$$\begin{bmatrix} I \\ L_0 \end{bmatrix} N_R \nu = \frac{dS}{dt} = \begin{bmatrix} dS_i/dt \\ dS_d/dt \end{bmatrix},$$

where the terms  $dS_i/dt$  and  $dS_d/dt$  refer to the independent and dependent rates of change, respectively. From the above equation, it can be shown that the relationship between the dependent and the independent species is given by:  $S_d(t) - S_d(0) = L_0 [S_i(t) - S_i(0)]$  for all time  $t$ . Introducing the constant vector  $T = S_d(0) - L_0 S_i(0)$ , and recalling that  $S = (S_i, S_d)$ , we can introduce  $\Gamma = [-L_0, I]$ , and write the vector  $T$  concisely as

$$\Gamma S = T.$$

$\Gamma$  is called the conservation matrix.

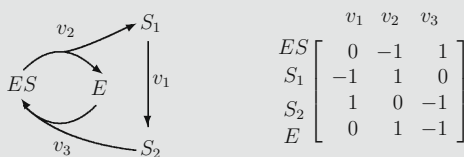
In the example shown in Fig. 13.2, the conservation matrix  $\Gamma$  can be shown to be

$$\Gamma = [1 \ 1].$$

A more complex example is illustrated in Box 1. Algorithms for evaluating the conservation constraints and the Link matrix can be found in (42, 14, 73, 85).

### Box 1. Conservation Analysis.

Consider the simple reaction network shown on the left below:



The **stoichiometry matrix** for this network is shown on the right. This network possesses two conserved cycles given by the constraints:  $S_1 + S_2 + ES = T_1$  and  $E + ES = T_2$ . The set of independent species includes  $\{ES, S_1\}$ , and the set of dependent species  $\{E, S_2\}$ .

The  $L_0$  matrix can be shown to be:

$$L_0 = \begin{bmatrix} -1 & -1 \\ -1 & 0 \end{bmatrix}.$$

The complete set of equations for this model is therefore:

$$\begin{bmatrix} S_2 \\ E \end{bmatrix} = \begin{bmatrix} -1 & -1 \\ -1 & 0 \end{bmatrix} \begin{bmatrix} ES \\ S_1 \end{bmatrix} + \begin{bmatrix} T_1 \\ T_2 \end{bmatrix}$$

$$\begin{bmatrix} dES/dt \\ dS_1/dt \end{bmatrix} = \begin{bmatrix} 0 & -1 & 1 \\ -1 & 1 & 0 \end{bmatrix} \begin{bmatrix} v_1 \\ v_2 \\ v_3 \end{bmatrix}.$$

Note that even though there appears to be four variables in this system, there are in fact only two independent variables,  $\{ES, S_1\}$ , and hence only two differential equations and two linear constraints.

An excellent source of material related to the analysis of the stoichiometry matrix can be found in the text book by Heinrich and Schuster (37) and more recently (53).

---

### 3. Biochemical Control Theory

The system **Eq. [1]** describes the time evolution of the network. This evolution can be characterized in three ways: **thermodynamic equilibrium** where all net flows are zero and no concentrations change in time; **steady state** where net flows of mass traverse the boundaries of the network and no concentrations change in time; and finally the **transient state** where flows and concentrations are both changing in time. Only the steady state and transient states are of real interest in biology. Steady states can be further characterized as stable or unstable, which will be discussed in a later section.

The steady-state solution for a network is obtained by setting the left-hand side of the system **Eq. [1]** to zero,  $Nv = 0$ , and solving for the concentrations. Consider the simplest possible model:



where we will assume that  $X_0$  and  $X_1$  are boundary species that do not change in time and that each reaction is governed by simple mass-action kinetics. With these assumptions we can write down the system equation for the rate of change of  $S_1$  as:

$$dS_1/dt = k_1 X_0 - k_2 S_1.$$

We can solve for the transient behavior of this system by integrating the system equation and setting an initial condition,  $S_1(0) = A_0$ , to yield:

$$S_1(t) = A_0 e^{-k_2 t} + \frac{k_1 X_0}{k_2} (1 - e^{-k_2 t}).$$

This equation describes how the concentration of  $S_1$  changes in time. The steady state can be determined either by letting  $t$  go to infinity or by setting the system equation to zero and solving for  $S_1$ ; either way, the steady-state concentration of  $S_1$  can be shown to be:

$$S_1 = \frac{k_1 X_0}{k_2}.$$

Although simple systems such as this can be solved analytically for both the time course evolution and the steady state, the method rapidly becomes unworkable for larger systems. The problem becomes particularly acute when, instead of simple mass-action kinetics, we begin to use enzyme kinetic rate laws that introduce nonlinearities into the equations. For all intent and purposes, analytical solutions for biologically interesting systems are unattainable. Instead one must turn to numerical solutions; however, numerical solutions are particular solutions, not general, which an analytical approach would yield. As a result, to obtain a thorough understanding of a model, many numerical simulations may need to be carried out. In view of these limitations many researchers apply small perturbation theory (linearization) around some operating point, usually the steady state. By analyzing the behavior of the system using small perturbations, only the linear modes of the model are stimulated and therefore the mathematics becomes tractable. This is a tried and tested approach that has been used extensively in many fields, particularly engineering, to deal with systems where the mathematics makes analysis difficult.

Probably, the first person to consider the linearization of biochemical models was Joseph Higgins at the University of Pennsylvania in the 1950s. Higgins introduced the idea of a “reflection coefficient” (40, 38), which described the relative change of one variable to another for small perturbations. In his Ph.D. thesis, Higgins describes many properties of the reflection coefficients and in later work, three groups, Savageau (75, 77), Heinrich and Rapoport (36, 35), and Kacser and Burns (9, 49) independently and simultaneously developed this work into what is now called Metabolic Control Analysis or Biochemical Systems Theory. These developments extended Higgins’ original ideas significantly and the formalism is now the theoretical foundation for describing deterministic, continuous models of biochemical networks. The theory has, in the past 20 years or so, been further developed with the most recent important advances by Ingalls (45) and Rao (68). In this chapter we will call this approach **Biochemical Control Theory**, or **BCT**.

### 3.1. Linear Perturbation Analysis

#### 3.1.1. Elementary Processes

The fundamental unit in biological networks is the chemical transformation. Such transformations vary, ranging from simple binding processes, transport processes, to more elaborate aggregated kinetics such as Michaelis-Menten and complex cooperative kinetics.



Traditionally, chemical transformations are described using a rate law. For example, the rate law for a simple irreversible Michaelis-Menten reaction is often given as

$$v = \frac{V_{\max} S}{K_m + S}, \quad [3]$$

where  $S$  is the substrate and the  $V_{\max}$  and  $K_m$  kinetic constants. Such rate laws form the basis of larger pathway models.

A fundamental property of any rate law is the so-called kinetic order, sometimes also called the reaction order. In simple mass-action chemical kinetics, the kinetic order is the power to which a species is raised in the kinetic rate law. Reactions with zero-order, first-order, and second-order are the common types of reactions found in chemistry, and in each case the kinetic order is zero, one, and two, respectively. It is possible to generalize the kinetic order as the scaled derivative of the reaction rate with respect to the species concentration, thus

$$\text{Elasticity Coefficient: } \varepsilon_S^v = \frac{\partial v}{\partial S} \frac{S}{v} = \frac{\partial \ln v}{\partial \ln S} \approx v\%/S\%.$$

When expressed this way, the kinetic order in biochemistry is called the *elasticity coefficient*. Applied to a simple mass-action rate law such as  $v = kS$ , we can see that  $\varepsilon_S^v = 1$ . For a generalized mass-action law such as

$$v = k \prod S_i^{n_i},$$

the elasticity for the  $i$ th species is simply  $n_i$ , that is, it equals the kinetic order. For aggregate rate laws such as the Michaelis-Menten rate law, the elasticity is more complex, for example, the elasticity for the rate law **Eq. [3]** is:

$$\varepsilon_S^v = \frac{K_m}{S + K_m}.$$

This equation illustrates that the kinetic order, though a constant for simple rate laws, is a variable for complex rate laws. In this particular case, the elasticity approaches unity at low substrate concentrations (first-order) and zero at high substrate concentrations (zero-order).

Elasticity coefficients can be defined for any effector molecule that might influence the rate of reaction, this includes substrates, products, inhibitors, activators, and so on. Elasticities are positive for substrates and activators, but negative for products and inhibitors.

At this point, elasticities might seem like curiosities and of no great value; left on their own, this might well be true. The real value of elasticities is that they can be combined into expressions that describe how the whole pathway responds collectively to perturbations. To explain this statement one must consider an additional measure, the control coefficient.

## 3.1.2. Control Coefficients

Unlike an elasticity coefficient, which describes the response of a single reaction to perturbations in its immediate environment, a control coefficient describes the response of a whole pathway to perturbations in the pathway's environment.

At steady state, a reaction network will sustain a steady rate called the flux, often denoted by the symbol,  $J$ . The flux describes the rate of mass transfer through the pathway. In a linear chain of reactions, the steady-state flux has the same value at every reaction. In a branched pathway, the flux divides at the branch points. The flux through a pathway can be influenced by a number of external factors, such as enzyme activities, rate constants, and boundary species. Thus, changing the gene expression that codes for an enzyme in a metabolic pathway will have some influence on the steady-state flux through the pathway. The amount by which the flux changes is expressed by the flux control coefficient.

$$C_{E_i}^J = \frac{dJ}{dE_i} \frac{E_i}{J} = \frac{d \ln J}{d \ln E_i} \approx J\% / E_i\%. \quad [4]$$

In the expression above,  $J$  is the flux through the pathway and  $E_i$  the enzyme activity of the  $i$ th step. The flux control coefficient measures the fractional change in flux brought about by a given fractional change in enzyme activity. Note that the coefficient as well as the elasticity coefficients are defined for small changes.

For a reaction pathway one can plot (**Fig. 13.3**) the steady-state flux,  $J$ , as a function of the activity of one of the enzymes. The flux control coefficient can be interpreted on this graph as the scaled slope of the response at a given steady state. Given that the curve is a function of the enzyme activity, it should be clear that the value of the control coefficient is also a function of enzyme activity and consequently the steady state. Control coefficients are not constants but vary according to the current steady state.

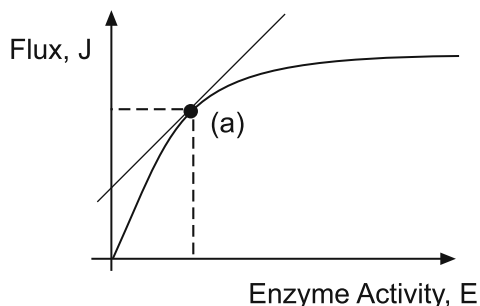


Fig. 13.3. Typical response of the pathway steady-state flux as a function of enzyme activity. The flux control coefficient is defined at a particular operating point, marked (a) on the graph. The value of the coefficient is measured by the scaled slope of the curve at (a).

One can also define a similar coefficient, the concentration control coefficient, with respect to species concentrations, thus:

$$C_{E_i}^S = \frac{dS}{dE_i} \frac{E_i}{S} = \frac{d \ln S}{d \ln E_i} \approx S\%/E_i\%. \quad [5]$$

### 3.1.3. Relationship Between Elasticities and Control Coefficients

One of the most significant discoveries made early on in the development of BCT (Biochemical Control Theory) was the existence of a relationship between the elasticities and the control coefficients. This enabled one, for the first time, to describe in a general way, how properties of individual enzymes could contribute to pathway behavior. More importantly, this relationship could be studied without the need to solve, analytically, the system **Eq. [1]**. Particular examples of these relationships will be given in the subsequent sections; here we will concentrate on the general relationship.

There are two related ways to derive the relationship between elasticities and control coefficients, the first is via the differentiation of the system **Eq. [1]** at steady state and the second by the connectivity theorem.

**System Equation Derivation.** The system equation can be written more explicitly to show its dependence on the enzyme activities (or any parameter set) of the system:  $N\mathbf{v}(s(\mathbf{E}), \mathbf{E}) = \mathbf{0}$ . By differentiating this expression with respect to  $\mathbf{E}$ , we obtain

$$\frac{d\mathbf{s}}{d\mathbf{E}} = - \left( N_R \frac{\partial \mathbf{v}}{\partial s} L \right)^{-1} N_R \frac{\partial \mathbf{v}}{\partial \mathbf{E}}. \quad [6]$$

The terms  $\partial \mathbf{v} / \partial s$  and  $\partial \mathbf{v} / \partial \mathbf{E}$  are unscaled elasticities [*See (69, 37, 43, 53)* for details of the derivation]. By scaling the equation with the species concentration and enzyme activity, the left-hand side becomes the concentration control coefficient expressed in terms of scaled elasticities. The flux control coefficients can also be derived by differentiating the expression:  $J = \mathbf{v}[s(\mathbf{p}), \mathbf{p}]$  to yield:

$$\frac{dJ}{d\mathbf{E}} = \left[ I - \frac{\partial \mathbf{v}}{\partial s} \left( N_R \frac{\partial \mathbf{v}}{\partial s} L \right)^{-1} N_R \right] \frac{\partial \mathbf{v}}{\partial \mathbf{E}}. \quad [7]$$

Again, the flux expression can be scaled by  $\mathbf{E}$  and  $J$  to yield the scaled flux control coefficients. These expressions, though unwieldy to some degree, are very useful for deriving symbolic expressions relating the control coefficients to the elasticities. A very thorough treatment together with the derivations of these equations and much more can be found in Hofmeyr 2001.

**Theorems.** Examination of expressions [6] and [7] yields some additional and unexpected relationships between the control coefficients and the elasticities, called the summation and connectivity theorems. These theorems were originally discovered by modeling small networks using an analog computer (Jim Burns, personal communication), but have since been derived by other means.

The **flux summation theorem** states that the sum of all the flux control coefficients in any pathway is equal to unity.

$$\sum_{i=1}^n C_i^J = 1$$

It is also possible to derive a similar relationship with respect to species concentrations, namely

$$\sum_{i=1}^n C_i^{S_k} = 0$$

In both relationships,  $n$ , is the number of reaction steps in the pathway. The flux summation theorem indicates that there is a finite amount of “control” (or sensitivity) in a pathway and implies that control is shared between all steps. In addition, it states that if one step were to gain control, then one or more other steps must lose control.

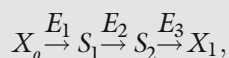
Arguably, the most important relationship is between the control coefficients and the elasticities.

$$\sum C_i^J \varepsilon_S^i = 0$$

This theorem, and its relatives (88, 19, 20), is called the **connectivity theorem** and is probably the most significant relationship in computational systems biology because it relates two different levels of description, the local level, in the form of elasticities, and the system level, in the form of control coefficients. Given the summation and connectivity theorems, it is possible to combine them and solve for the control coefficients in terms of the elasticities. For small networks this approach is a viable way to derive the relationships (19), especially when combined with software such as MetaCon (81), which can compute the relationships algebraically. Box 2 illustrates a simple example of this method.

### Box 2. Using Theorems to Derive Control Equations

Consider the simple reaction network, comprising three enzyme-catalyzed reactions, shown below:



where,  $X_o$  and  $X_1$  are fixed boundary species. The flux summation theorem can be written down as:

$$C_{E_1}^J + C_{E_2}^J + C_{E_3}^J = 1,$$

while the two connectivity theorems, one centered around each species, are given by:

$$C_{E_1}^J \varepsilon_1^1 + C_{E_2}^J \varepsilon_1^2 = 0$$

$$C_{E_2}^J \varepsilon_2^2 + C_{E_3}^J \varepsilon_2^3 = 0.$$

These three equations can be recast in matrix form as:

$$\begin{bmatrix} 1 & 1 & 1 \\ \varepsilon_1^1 & \varepsilon_1^2 & 0 \\ 0 & \varepsilon_2^2 & \varepsilon_2^3 \end{bmatrix} \begin{bmatrix} C_{E_1}^J \\ C_{E_2}^J \\ C_{E_3}^J \end{bmatrix} = \begin{bmatrix} 1 \\ 0 \\ 0 \end{bmatrix}$$

The matrix equation can be rearranged to solve for the vector,  $[C_{E_1}^J C_{E_2}^J C_{E_3}^J]^T$ , by inverting the elasticity matrix, to yield:

$$C_{E_1}^J = \frac{\varepsilon_1^2 \varepsilon_2^3}{\varepsilon_1^1 \varepsilon_2^2 - \varepsilon_1^1 \varepsilon_2^3 + \varepsilon_1^2 \varepsilon_2^3}$$

$$C_{E_2}^J = \frac{-\varepsilon_1^1 \varepsilon_2^3}{\varepsilon_1^1 \varepsilon_2^2 - \varepsilon_1^1 \varepsilon_2^3 + \varepsilon_1^2 \varepsilon_2^3}$$

$$C_{E_3}^J = \frac{-\varepsilon_1^1 \varepsilon_2^2}{\varepsilon_1^1 \varepsilon_2^2 - \varepsilon_1^1 \varepsilon_2^3 + \varepsilon_1^2 \varepsilon_2^3}$$

Further details of the procedure can be found in (19, 20). For larger systems **Eq. [7]** can be used in conjunction with software tools such as Maple, bearing in mind that **Eq. [7]** yields unscaled coefficients.

### 3.2. Linear Analysis of Pathway Motifs

In the following sections we will describe the application of BCT to some basic and common motifs found in cellular networks. These include, straight chains, branches, cycles, and feedback loops.

#### 3.2.1. Straight Chains

Although linear sequences of reaction steps are actually quite rare in cellular networks (most networks are so heavily branched that uninterrupted sequences are quite uncommon), their study can reveal some basic properties that are instructive to know.

One of the oldest concepts in cellular regulation is the notion of the rate-limiting step. It was Blackman in 1905 (6) who wrote the famous phrase: ‘when a process is conditioned as to its rapidity by a number of separate factors, the rate of the process is limited by the pace of the slowest factor’. It was this statement that started a century long love-affair with the idea of the rate-limiting step in biochemistry, a concept that has lasted to this very day. From the 1930s to the 1950s, there were, however, a number of published

papers which were highly critical of the concept, most notably Burton (11), Morales (62) and Hearon (33) in particular. Unfortunately, much of this work did not find its way into the rapidly expanding fields of biochemistry and molecular biology after the second world war, and instead the intuitive idea first pronounced by Blackman still remains today one of the basic but erroneous concepts in cellular regulation. This is more surprising because a simple quantitative analysis shows that it cannot be true, and there is ample experimental evidence (34, 10) to support the alternative notion, that of shared control.

The confusion over the existence of rate-limiting steps stems from a failure to realize that rates in cellular networks are governed by the law of mass-action, that is, if a concentration changes, then so does its rate of reaction. Many researchers try to draw analogies between cellular pathways and human experiences such as traffic congestion on freeways or customer lines at shopping store check-outs. In each of these analogies, the rate of traffic and the rate of customer checkouts does not depend on how many cars are in the traffic line or how many customers are waiting. Such situations warrant the correct use of the phrase rate-limiting step. Traffic congestion and the customer line are rate-limiting because the only way to increase the flow is to either widen the road or increase the number of cash tills, that is, there is a single factor which determines the rate of flow. In reaction networks, flow is governed by many factors, including the capacity of the reaction ( $V_{max}$ ) and substrate/ product/effector concentrations. In biological pathways, rate-limiting steps are therefore the exception rather than the rule. Many hundreds of measurements of control coefficients have borne out this prediction. A simple quantitative study will also make this clear.

Consider a simple linear sequence of reactions governed by reversible mass-action rate laws:



where  $X_0$  and  $X_n$  are fixed boundary species so that the pathway can sustain a steady state. If we assume the reaction rates to have the simple form:

$$v_j = k_j \left( S_j - \frac{S_{j+1}}{q_j} \right),$$

where  $q_j$  is the thermodynamic equilibrium constant and  $k_j$  the forward rate constant, we can compute the steady state flux,  $J$ , to be (37):

$$J = \frac{X_0 \prod_{j=1}^n q_j - X_n}{\sum_{l=1}^n 1/k_l \prod_{j=l}^n q_j}.$$

By modifying the rate laws to include an enzyme factor, such as:  $v_j = E_j k_j \left( S_j - \frac{S_{j+1}}{q_j} \right)$ , we can also compute the flux control coefficients as (37):

$$C_i^J = \frac{1/k_i \prod_{j=i}^n q_j}{\sum_{l=1}^n 1/k_l \prod_{j=l}^n q_j}.$$

Both equations show that the ability of a particular step to limit the flux is governed not only by the particular step itself but also by *all* other steps. Prior to the 1960s, this was a well-known result (62, 33), but was subsequently forgotten with the rapid expansion of biochemistry and molecular biology. The control coefficient equation also puts limits on the values for the control coefficients in a linear chain, namely  $0 \leq C_i^J \leq 1$  and

$$\sum_{i=1}^n C_i^J = 1,$$

which is the flux control coefficient summation theorem. In a linear pathway the control of flux is therefore most likely to be distributed among all steps in the pathway. This simple study shows that the notion of the rate-limiting step is too simplistic and a better way to describe a reaction's ability to limit flux is to state its flux control coefficient.

Although a linear chain puts bounds on the values of the flux control coefficients, branched systems offer no such limits. It is possible that increases in enzyme activity in one limb can decrease the flux through another, hence the flux control coefficient can be negative. In addition, it is possible for the flux control coefficient to be greater than unity (**Note 3**).

### 3.2.2. Branched Systems

Branching structures in metabolism are probably one of the most common metabolic patterns. Even a pathway such as glycolysis, often depicted as a straight chain in textbooks, is in fact a highly branched pathway.

A linear perturbation analysis of a branched pathway can reveal some interesting potential behavior. Consider the following simple branched pathway (**Fig. 13.4**):

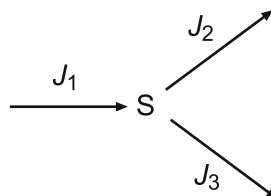


Fig. 13.4. A simple branched pathway. This pathway has three different fluxes,  $J_1$ ,  $J_2$ , and  $J_3$ , which at steady state are constrained by  $J_1 = J_2 + J_3$ .

where  $J_i$  are the steady state fluxes. By the law of conservation of mass, at steady state, the fluxes in each limb are governed by the relationship:

$$J_1 - (J_2 + J_3) = 0.$$

In terms of control theory, there will be four sets of control coefficients, one concerned with changes in the intermediate, S, and three sets corresponding to each of the individual fluxes.

Let the fraction of flux through  $J_2$  be given by  $\alpha = J_2/J_1$  and the fraction of flux through  $J_3$  be  $1 - \alpha = J_3/J_1$ . The flux control coefficients for step two and three can be derived and shown to be equal to (19):

$$C_{E_2}^{J_2} = \frac{\varepsilon_1 - \varepsilon_3(1 - \alpha)}{\varepsilon_1 - \varepsilon_2\alpha - \varepsilon_3(1 - \alpha)} > 0 \quad C_{E_3}^{J_2} = \frac{\varepsilon_2(1 - \alpha)}{\varepsilon_1 - \varepsilon_2\alpha - \varepsilon_3(1 - \alpha)} < 0.$$

Note that the flux control coefficient  $C_{E_3}^{J_2}$  is negative, indicating that changes in the activity of  $E_3$  decrease the flux in the other limb. To understand the properties of a branched system, it is instructive to look at different flux distributions. For example, consider the case when the bulk of flux moves down  $J_3$  and only a small amount goes through the upper limb  $J_2$ , that is,  $\alpha \rightarrow 0$  and  $1 - \alpha \rightarrow 1$  (See Fig. 13.5b). Let us examine how the small amount of flux through  $J_2$  is influenced by the two branch limbs,  $E_2$  and  $E_3$ .

$$C_{E_2}^{J_2} \rightarrow \frac{\varepsilon_1 - \varepsilon_3}{\varepsilon_1 - \varepsilon_3} = 1.$$

$$C_{E_3}^{J_2} \rightarrow \frac{\varepsilon_2}{\varepsilon_1 - \varepsilon_3}.$$

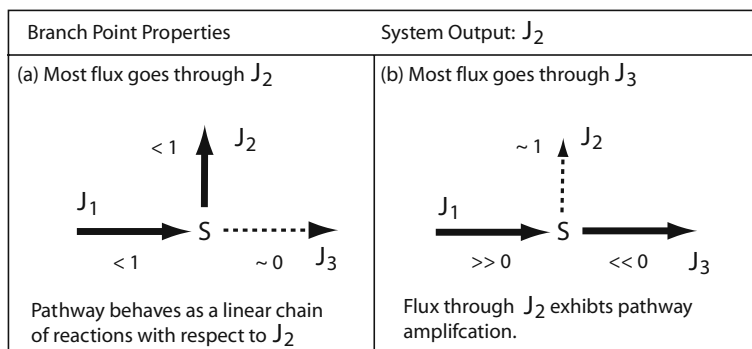


Fig. 13.5. The figure shows two flux extremes relative to the flux through branch  $J_2$ . In case (a) where most of the flux goes through  $J_2$ , the branch reverts functionally to a simple linear sequence of reactions comprising  $J_1$  and  $J_2$ . In case (b), where most of the flux goes through  $J_3$ , the flux through  $J_2$  now becomes very sensitive to changes in activity at  $J_1$  and  $J_3$ . Given the right kinetic settings, the flux control coefficients can become “ultrasensitive” with values greater than one (less than minus one for activity changes at  $J_3$ ). The values next to each reaction indicates the flux control coefficient for the flux through  $J_2$  with respect to activity at the reaction.



The first thing to note is that  $E_2$  tends to have proportional influence over its own flux. Since  $J_2$  carries only a very small amount of flux, any changes in  $E_2$  will have little effect on  $S$ , hence the flux through  $E_2$  is almost entirely governed by the activity of  $E_2$ . Because of the flux summation theorem and the fact that  $C_{E_2}^{J_2} = 1$ , the remaining two coefficients must be equal and opposite in value. Since  $C_{E_3}^{J_2}$  is negative,  $C_{E_1}^{J_2}$  must be positive. Unlike a linear chain, the values for  $C_{E_2}^{J_2}$  and  $C_{E_1}^{J_2}$  are not bounded between zero and one and depending on the values of the elasticities it is possible for the control coefficients to greatly exceed one (48, 55). It is conceivable to arrange the kinetic constants so that every step in the branch has a control coefficient of unity (one of which must be -1). Using the old terminology, we would conclude from this that every step in the pathway is the rate-limiting step.

Let us now consider the other extreme, when most of the flux is through  $J_2$ , that is  $\alpha \rightarrow 0$  and  $1 - \alpha \rightarrow 0$  (See Fig. 13.5a). Under these conditions the control coefficients yield:

$$C_{E_2}^{J_2} \rightarrow \frac{\varepsilon_1}{\varepsilon_1 - \varepsilon_2}$$

$$C_{E_3}^{J_2} \rightarrow 0$$

In this situation the pathway has effectively become a simple linear chain. The influence of  $E_3$  on  $J_2$  is negligible. Figure 13.5 summarizes the changes in sensitivities at a branch point.

### 3.2.3. Cyclic Systems

Cyclic systems are extremely common in biochemical networks; they can be found in metabolic, genetic, and particularly signaling pathways. The functional role of cycles is not however fully understood, although in some cases their operational function is beginning to become clear. We can use linear perturbation analysis to uncover some of the main properties of cycles.

Figure 13.6 illustrates two common cyclic structures found in signaling pathways. Such cycles are often formed by a combination of a kinase and a phosphatase. In many cases only one of the molecular species is active. For example, in Fig. 13.6a, let us assume that  $S_2$  is the active (output) species, while in Fig. 13.6b,  $S_3$  is the active (output) species. In a number of cases one observes multiple cycles formed by multi-site phosphorylation. Figure 13.6b shows a common two-stage multi-site cycle. Note that in each case, the cycle steady-state is maintained by the turnover of ATP. One question that can be addressed is how the steady-state output of each cycle,  $S_2$  and  $S_3$ , depends on the input stimulus,  $S$ . This stimulus is assumed to be a stimulus of the kinase activity.

One approach to this is to build a detailed kinetic model and solve for the steady-state concentration of  $S_2$  and  $S_3$  as a function of  $S$ . This has been done analytically in a few cases (30, 31), but requires the modeler to choose a particular kinetic model for the

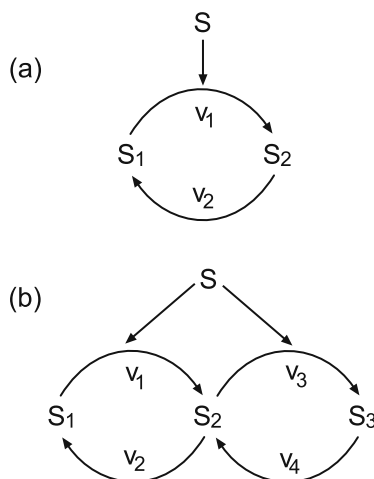


Fig. 13.6. Two common cyclic motifs found in signaling pathways. (a) Single covalent modification cycle,  $S_2$  is the active species,  $S$  is the stimulus; (b) Double cycle with  $S_3$  the active species,  $S$  is the stimulus.

kinase and phosphatase steps. A perturbation analysis based on BCT need only be concerned with the response characteristics of the kinase and phosphatase steps, not the details of the kinetic mechanism. The response of  $S_2$  to changes in the stimulus  $S$  can be shown to be given by the expression (79, 74):

$$C_S^{S_2} = \frac{M_1}{\varepsilon_1^1 M_2 + \varepsilon_2^2 M_1},$$

where  $C_S^{S_2}$  is the control coefficient of  $S_2$  with respect to  $S$ .  $M_1$  and  $M_2$  are the mole fractions of  $S_1$  and  $S_2$ , respectively, and  $\varepsilon_1^1$  the elasticity of  $v_1$  with respect to  $S_1$  and  $\varepsilon_2^2$  the elasticity of  $v_2$  with respect to  $S_2$ . If kinase and phosphatase are operating below saturation, then the elasticities will equal one,  $\varepsilon_1^1 = 1$  and  $\varepsilon_2^2 = 1$ ; therefore, the response of  $S_2$  to  $S$  is simply given by the mole fraction  $M_1$ , which means that the response is bounded between zero and one. This situation is equivalent to the non-ultrasensitive response, sometimes termed the hyperbolic response (31).

In contrast, if the kinase and phosphatase operate closer to saturation, such that the elasticities are much smaller than one, then the denominator in the response equation can be less than the numerator and the control coefficient can exceed one. This situation is representative of zero-order ultrasensitivity and corresponds to the well-known sigmoid response (31). Thus without any reference to detailed kinetic mechanisms, it is possible to uncover the ultrasensitive behavior of the network. We can carry out the same kind of analysis on the dual cycle, **Fig. 13.6b**, to derive the following expression for  $C_S^{S_3}$ :

$$C_S^{S_3} = \frac{S_1(\varepsilon_2^3 + \varepsilon_2^2) + S_2\varepsilon_1^1}{\varepsilon_2^3\varepsilon_3^4 S_1 + \varepsilon_1^1\varepsilon_3^4 S_2 + \varepsilon_1^1\varepsilon_3^3 S_3}.$$

If we assume linear kinetics on each reaction such that all the elasticities equal one, the equation simplifies to

$$C_S^{S_3} = \frac{2S_1 + S_2}{S_1 + S_2 + S_3}.$$

This shows that given the right ratios for  $S_1$ ,  $S_2$ , and  $S_3$ , it is possible for  $C_S^{S_3} > 1$ . Therefore, unlike the case of a single cycle where near saturation is required to achieve ultrasensitivity, multiple cycles can achieve ultrasensitivity with simple linear kinetics (See Fig. 13.7).

The cyclic models considered here assume negligible sequestration of the cycle species by the catalyzing kinase and phosphatase. In reality, this is not likely to be the case because experimental evidence indicates that the concentrations of the catalyzing enzymes and cycle species are comparable [See (8) for a range of illustrative data]. In such situations additional effects are manifest (21, 72), of particular interest is the emergence of new regulatory feedback loops, which can alter the behavior quite markedly (See 60, 64).

#### 3.2.4. Negative Feedback

A common regulatory motif found in cellular networks is the negative feedback loop (Fig. 13.8). Feedback has the potential to confer many interesting properties on a pathway, with homeostasis probably being the most well known. In this chapter we do not have space to cover all the effects of negative feedback and will focus instead on two properties, homeostasis and instability; however, more details can be found in (74). Using BCT it is easy to show the effect of negative feedback on a pathway.

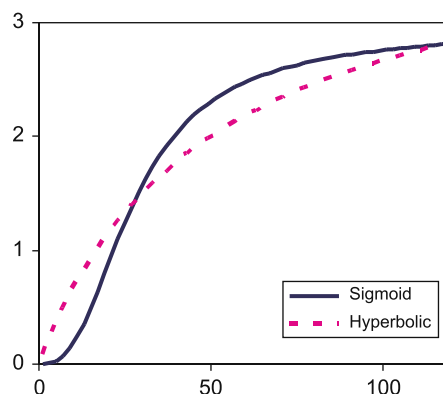


Fig. 13.7. Steady-state responses for the cycles shown in Fig. 13.6. The simplest cycle **6(a)** shows a hyperbolic response when the kinase and phosphatase operate below saturation (dotted line). The double cycle **6(b)** shows more complex behavior in the form of a sigmoid response, the kinetics again operating below saturation (solid line). This shows that zero-order kinetics is not a necessary condition of ultrasensitivity.

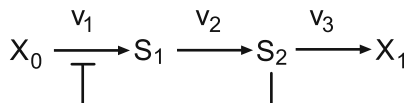


Fig. 13.8. Simple negative feedback loop.  $v_1$ ,  $v_2$ , and  $v_3$  are the reaction rates.  $S_2$  acts to inhibit its own production by inhibition of  $v_1$ .

The flux control coefficients for the three steps in **Fig. 13.8** are shown below (77, 48). To aid comparison, the left-hand equations show the equations with feedback while the right-hand equations have been derived assuming no feedback. The feedback term is represented by a single elasticity term,  $\varepsilon_2^1$ . This elasticity measures the strength of the feedback and has a negative value, indicating that changes in  $S_2$  result in decreases in the reaction rate of  $v_1$ . For cooperative enzymes, the elasticity may also have values less than  $-1$ .

With Feedback	Without Feedback
$C_{E_1}^J = \frac{\varepsilon_1^2 \varepsilon_2^3}{\varepsilon_1^2 \varepsilon_2^3 - \varepsilon_1^1 \varepsilon_2^3 + \varepsilon_1^1 \varepsilon_2^2 - \varepsilon_1^2 \varepsilon_2^1}$	$C_{E_1}^J = \frac{\varepsilon_1^2 \varepsilon_2^3}{\varepsilon_1^2 \varepsilon_2^3 - \varepsilon_1^1 \varepsilon_2^3 + \varepsilon_1^1 \varepsilon_2^2}$
$C_{E_2}^J = \frac{-\varepsilon_1^1 \varepsilon_2^3}{\varepsilon_1^2 \varepsilon_2^3 - \varepsilon_1^1 \varepsilon_2^3 + \varepsilon_1^1 \varepsilon_2^2 - \varepsilon_1^2 \varepsilon_2^1}$	$C_{E_2}^J = \frac{-\varepsilon_1^1 \varepsilon_2^3}{\varepsilon_1^2 \varepsilon_2^3 - \varepsilon_1^1 \varepsilon_2^3 + \varepsilon_1^1 \varepsilon_2^2}$
$C_{E_3}^J = \frac{\varepsilon_1^1 \varepsilon_2^2 - \varepsilon_1^2 \varepsilon_2^1}{\varepsilon_1^2 \varepsilon_2^3 - \varepsilon_1^1 \varepsilon_2^3 + \varepsilon_1^1 \varepsilon_2^2 - \varepsilon_1^2 \varepsilon_2^1}$	$C_{E_3}^J = \frac{\varepsilon_1^1 \varepsilon_2^2}{\varepsilon_1^2 \varepsilon_2^3 - \varepsilon_1^1 \varepsilon_2^3 + \varepsilon_1^1 \varepsilon_2^2}$

The first difference to notice in the equations is that the denominator, though remaining positive in value, has an additional term compared to the system without feedback,  $\varepsilon_1^2 \varepsilon_2^1$ . This additional term includes the elasticity of the feedback mechanism.

The numerators for  $E_1$  and  $E_2$  are both unaffected by the feedback. However, because the denominator has an additional positive term, the ratio of numerator to denominator in both cases must be smaller. The flux control coefficients for  $E_1$  and  $E_2$  are therefore reduced in the presence of feedback.

This result might appear at first glance counter-intuitive, surely the “controlled” step must have more “control” (as many undergraduate textbooks will assert)? Closer inspection, however, will reveal a simple explanation. Suppose the concentrations of either  $E_1$  or  $E_2$  are increased. This will cause the concentration of the signal metabolite  $S_2$  to increase. An increase in  $S_2$  will have two effects: the first is to increase the rate of the last reaction step, the second will inhibit the rate through  $E_1$ . The result of this is that the rate increase originally achieved by the increase in  $E_1$  or  $E_2$  will be reduced by the feedback. Therefore, compared to the non-feedback pathway, both enzymes  $E_1$  and  $E_2$  will have less control over the pathway flux. In addition, the greater the feedback elasticity,  $\varepsilon_2^1$  the smaller the control coefficients,  $C_{E_1}^J$ ,  $C_{E_2}^J$ . Thus the stronger the feedback, the less “control” the  $E_1$  and  $E_2$  have over the flux.

What about the flux control coefficient distal to the feedback signal,  $C_{E_3}^J$ ? According to the summation theorem, which states that the sum of the flux control coefficients of a pathway must sum to unity, if some steps experience a reduction in control, then other steps must acquire control. If the flux control of the first two steps decline, then it must be the case that control at the third step must increase. Examination of the third control coefficient equation reveals that as the feedback elasticity ( $\varepsilon_2^1$ ) strengthens, then  $C_{E_3}^J$  approaches unity, that is, the last step of the feedback system acquires most of the control.

For drug companies wishing to target pathways, this simple analysis would suggest that the best place to target a drug would be the steps distal to a controlling signal. Traditionally, many have believed it to be the controlled step that should be targeted; however, this analysis indicates that the controlled step is the worst step to target, since it has the least effect on the system. This argument assumes that the targeting does not affect the strength of the feedback itself.

As mentioned previously, one of the most well-known effects of negative feedback is to enhance homeostasis. In this case homeostasis refers to the stabilization of the end product  $S_2$ . We can examine the effect of negative feedback on the homeostasis of  $S_2$  by writing down the concentration control coefficient for  $C_{E_3}^{S_2}$

$$C_{E_3}^{S_2} = \frac{\varepsilon_1^1 - \varepsilon_1^2}{\varepsilon_1^2 \varepsilon_2^3 - \varepsilon_1^1 \varepsilon_2^3 + \varepsilon_1^1 \varepsilon_2^2 - \varepsilon_1^2 \varepsilon_2^1}.$$

Note that the numerator is unaffected by the presence of the feedback, whereas the denominator has an additional positive term originating from the feedback mechanism. This means that the feedback decreases the sensitivity of end product,  $S_2$ , with respect to the distal step,  $E_3$ . The effect of the feedback is to stabilize the end product concentration in the face of changing demand from distal steps. This allows a pathway to satisfy the changing demand characteristics of a subsystem distal to the negative feedback loop. We see such an arrangement in many metabolic pathways, clear examples include glycolysis, where demand is measured by ATP consumption, or amino biosynthesis, where demand is protein synthesis. In both cases one could imagine that it is important for the demand system, energy consumption and protein production, to be unimpeded by supply restraints.

Negative feedback therefore has the important task of matching different cellular systems. Hofmeyr and Cornish-Bowden (44) have written extensively on this topic, which they call supply-demand analysis. Interfacing different cellular modules using negative feedback, particularly in signalling pathways, is also discussed in (74).

Only a simple feedback loop has been considered here; for readers who are interested in a more exhaustive analysis, the work by Savageau and co-workers (76, 77, 2) is highly recommended. Moreover, feed-forward negative loops have recently been found to be a common motif and further details can be found in (59).

### 3.3. Relationship to Engineering Control Theory

In engineering there is much emphasis on questions concerning the stability and performance of technological systems. Over the years, engineers have developed an elaborate and general theory of control, which is applicable to many different technological systems. It is therefore the more surprising that engineering control theory has had little impact on understanding control systems found in biological networks. Part of the problem is related to the rich terminology and abstract nature of some of the mathematics that engineers use, this in turn makes the connection to biological systems difficult to see. This also partly explains why the biological community developed its own theory of control in the form of BCT. Until recently, there was little appreciation of what, if any connection, existed between these two approaches. It turns out the connection is rather more direct any anyone expected. The work by Ingalls (45) in particular [but also (68)], showed that the control coefficients in BCT and the transfer functions used so often in engineering are one and the same thing. This means that much of the machinery of engineering control theory, rather than being perhaps unrelated to biology, can in fact be transferred directly to biological problems.

Following Ingalls (45), let us write down the system equation in the following form:

$$\frac{d\mathbf{s}}{dt} = N\mathbf{v}(s, \mathbf{p}).$$

This equation can be linearized around a suitable operating point such as a steady state to obtain the linearized equation:

$$\frac{d\mathbf{x}}{dt} = \left[ N_R \frac{\partial \mathbf{v}}{\partial s} L \right] \mathbf{x}(t) + \left[ N_R \frac{\partial \mathbf{v}}{\partial \mathbf{p}} \right] \mathbf{u}(t). \quad [8]$$

This equation describes the rate of change of a perturbation  $\mathbf{x}$  around the steady state. For a stable system, the perturbation  $\mathbf{x}$  will decay toward the steady state and  $\mathbf{x}(t)$  will thus tend to zero. The linearized equation has the standard state space form commonly used in engineering control theory, that is

$$\frac{d\mathbf{x}}{dt} = A\mathbf{x}(t) + B\mathbf{u}(t),$$

with

$$A = N_R \frac{\partial \mathbf{v}}{\partial s} L \quad \text{and} \quad B = N_R \frac{\partial \mathbf{v}}{\partial \mathbf{p}}, \quad [9]$$

$u(t)$  is the input vector to the system, and may represent a set of perturbations in boundary conditions, kinetic constants, or depending on the particular model, gene expression changes.

Because of its equivalence to the state space form, **Eq. [8]** marks the entry point for describing biological control systems using the machinery of engineering control theory. In the following sections two applications, frequency analysis and stability analysis, will be presented, which apply engineering control theory, rephrased using BCT, to biological problems.

### 3.3.1. Frequency Response

It has been noted previously (3) that chemical networks can act as signal filters, that is, amplify or attenuate specific varying inputs. It may be the case that the ability to filter out specific frequencies has biological significance; for example, a cell may receive many different varying inputs that enter a common signaling pathway; signals that have different frequencies could be identified. In addition, multiple signals could be embedded in a single chemical species (such as  $Ca^{2+}$ ) and demultiplexed by different target systems. Finally, gene networks tend to be sources of noisy signals that may interfere with normal functioning; one could imagine specific control systems that reduce the noise using high frequency filtering (15).

In steady state, sinusoidal inputs to a linear or linearized system generate sinusoidal responses of the same frequency but of differing amplitude and phase. These differences are a functions of frequency. For a more detailed explanation, Ingalls (45) provides a readable introduction to concept of the frequency response of a system in a biological context.

Whereas the linearized **Eq. [8]** describes the evolution of the system in the time domain, the frequency response must be determined in the frequency domain. Mathematically there is a standard approach, called the Laplace transform, to moving a time domain representation into the frequency representation. By taking the ratio of the Laplace transform of the output to the transform of the input, one can derive the transfer function, which is a complex expression describing the relationship between the input and the output in the frequency domain. The change in the amplitude between the input and output is calculated by taking the absolute magnitude of the transfer function. The phase shift that indicates how much the output signal has been delayed can be computed by computing the phase angle. Note that under a linear treatment, the frequency does not change.

In biological systems the outputs are often the species concentrations or fluxes while the inputs are parameters such as kinetic constants, boundary conditions, or gene expression levels. By

taking the Laplace transform of **Eq. [8]** one can generate its transfer function (45, 68) The transfer function for the species vector  $s$  with respect to a set of parameters  $p$  is given by:

$$\mathbf{R}_p^s(w) = \left( iw\mathbf{I} - N_R \frac{\partial v}{\partial s} L \right)^{-1} N_R \frac{\partial v}{\partial p}. \quad [10]$$

The response at zero frequency is given by

$$\mathbf{R}_p^s(0) = - \left( N_R \frac{\partial v}{\partial s} L \right)^{-1} N_R \frac{\partial v}{\partial p}.$$

Comparison of the above equation with the concentration control coefficient Equation [6] shows they are equivalent. This is the most important result because it links classical control theory directly with BCT. Moreover, it gives a biological interpretation to the transfer functions so familiar to engineers. The transfer functions can be interpreted as a sensitivity of the amplitude and phase of a signal to perturbations in the input signal. The control coefficients of BCT are the transfer functions computed at zero frequency. Moreover, the denominator term in the transfer functions can be used to ascertain the stability of the system, a topic that will be covered in a later section.

**Frequency Analysis of Simple Linear Reaction Chains.** The simplest example to consider for a frequency analysis is a two-step pathway, that can be represented as a single gene expressing a protein that undergoes degradation (**Fig. 13.9**). This simple system has been considered previously by Arkin (3) who used a conventional approach to compute the response. Here we will use the BCT approach, which allows us to express the frequency response in terms of elasticities. Using **Eq. [10]** and assuming that the protein concentration has no effect on its synthesis, we can derive the following expression:

$$C_G^p = \frac{1}{\varepsilon_p^D + iw},$$

where  $\varepsilon_p^D$  is the elasticity for protein degradation with respect to the protein concentration.  $i$  is the complex number and  $w$ , the frequency input. At zero frequency ( $w = 0$ ) the equation reduces to the traditional control coefficient.

The frequency response of the simple network shown in **Fig. 13.9** is given in **Fig. 13.10**. This response shows a classic low-pass filter response, where at low frequencies the response is high and as the frequency increases the response of the system falls off. The explanation for this is straight forward; at high frequencies, kinetic mechanisms are simply too sluggish to respond fast enough to a rapidly changing signal and the system is unable to pass the input to the output (**Fig. 13.10**).



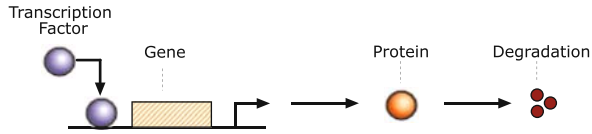


Fig. 13.9. Simple genetic circuit that can act as a low-pass filter.

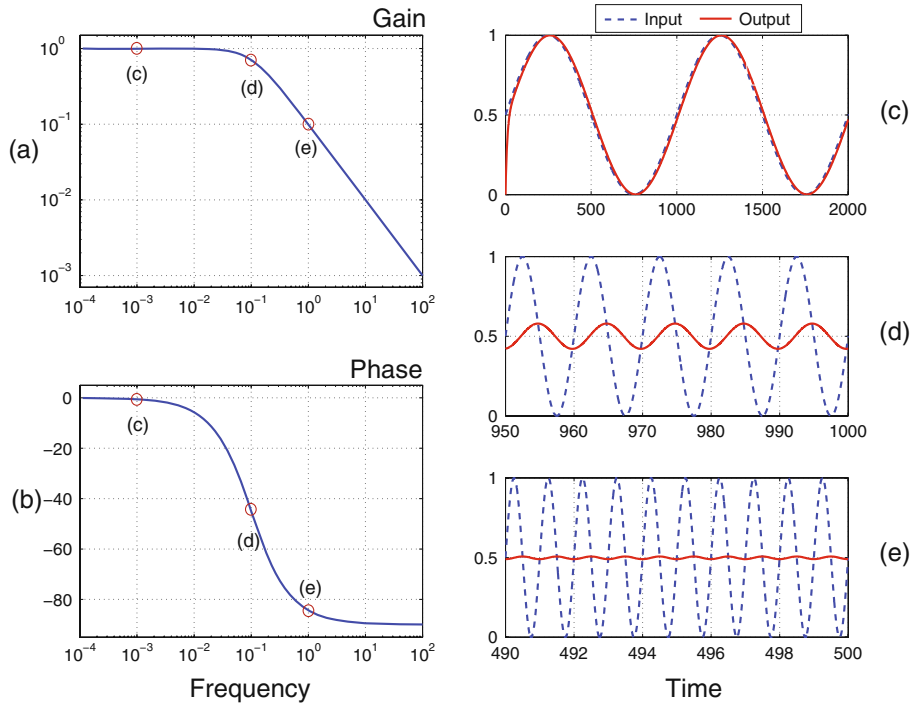


Fig. 13.10. Low-pass frequency response of the simple genetic circuit, **Fig. 13.9**. The two plots on the left indicate the amplitude and phase response, respectively. The three plots on the right show in each case the input signal and corresponding output signal. Each plot on the right was computed at a different frequency; these frequencies are indicated by the marked circles on the plots on the left.

If we cascade a series of genes one after the other (**Fig. 13.11**), the effect is simply to increase the attenuation so that even moderate frequencies are filtered out.

The unscaled response equation for the model shown in **Fig. 13.11** is given by

$$C_{v_1}^{S_3} = \frac{(\tilde{\epsilon})^n \tilde{\epsilon}_p}{(i\omega + \tilde{\epsilon})^n},$$

where the tilde,  $\tilde{\sim}$ , indicates an unscaled elasticity.  $n$  equals the number of genetic stages. We assume that all the elasticities are equal in value.

Many simple systems behave as low-pass filters because physically they are unable to respond fast enough at higher frequencies. Chemical systems are not unusual in this respect. It is possible however

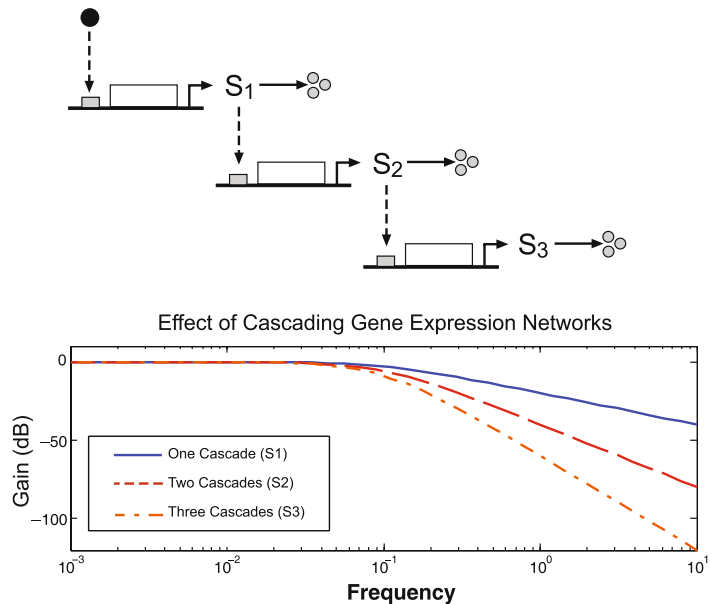


Fig. 13.11. Cascade of simple genetic circuits. See Fig. 13.9 for symbolism. The graph shows the frequency response as the cascade grows in stages. The more stages the greater the attenuation.

through added regulation to change the frequency response. In the paper by Paladugu (65) examples of networks exhibiting a variety of frequency responses are given, including high-pass and band-pass filters. In the next section we will consider how negative feedback can significantly change the frequency response.

**Frequency Analysis of a Simple Negative Feedback.** In earlier discussions on the effect of negative feedback, the analysis focused on the response to step perturbations on the steady state, effectively the response at zero frequency in the frequency response curve. Here we wish to investigate the frequency response across the entire frequency range.

**Figure 13.12** shows the frequency response for the simple network shown in **Fig. 13.8**. The figure includes two graphs, one computed with negative feedback and another without feedback. Without feedback the pathway operates as a simple low-pass filter (Solid line). With feedback (Dotted line), the frequency response is different. As expected, the response at low frequencies is attenuated, which reflects the homeostatic properties of the pathway. What is more interesting is the increase in responsiveness at higher frequencies, that is, the system becomes more sensitive to disturbances over a certain frequency range. This suggests that negative feedback adds a degree of resonance to the system and, given the right conditions, can cause the system to become unstable and

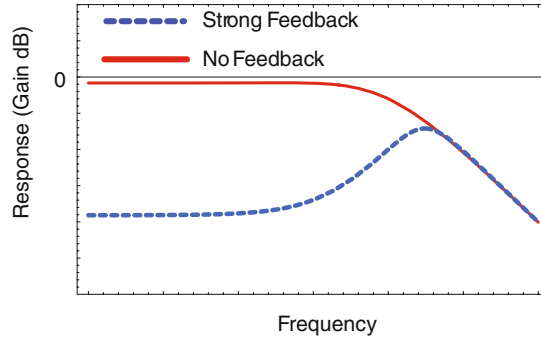


Fig. 13.12. Frequency response of end product  $S_2$  with respect to the input species  $X_0$  for a model of the kind shown in Fig. 13.8.

spontaneously oscillate. The shift in sensitivity to higher frequencies as a result of negative feedback has been observed experimentally in synthetic networks (4).

### 3.3.2. Stability Analysis

The stability of a system is the response it has to a disturbance to its internal state. Such disturbances can arise as a result of stochastic fluctuations in the concentrations of species or as external disturbances that impose changes on the internal species. If the system recovers to the original state after a disturbance, then it is classed as **stable**; if the system diverges, then it is classed as **unstable**. An excellent review by Jorg Stucki that focuses on stability in biochemical systems can be found in (80).

Consider the simple pathway shown in Eq. [2]. The differential equation for this simple pathway is given by

$$dS_1/dt = k_1 X_0 - k_2 S_1. \quad [11]$$

It can easily be shown that disturbances to  $S_1$  are stable. At steady state,  $dS_1/dt = 0$ ; thus by making a small disturbance,  $\delta S_1$  in  $S_1$  we can compute the effect this has on the rate of change of  $\delta S_1$  to be:

$$d(\delta S_1)/dt = -k_2 \delta S_1. \quad [12]$$

This shows that after the initial disturbance, the disturbance itself declines exponentially to zero; in other words, the system returns to the original steady state and the system is therefore stable. By dividing both sides by  $\delta S_1$  and taking the limit to infinitesimal changes, one can show (53) that the term,  $-k_2$ , is equal to,  $\partial d(S_1/dt)/\partial S_1$ . The stability of this simple system can therefore be determined by inspecting the sign of  $\partial d(S_1/dt)/\partial S_1$ .

Now consider a change to the kinetic law,  $k_1 X_o$ , governing the first reaction. Instead of simple linear kinetics let us use a cooperative enzyme which is activated by the product  $S_I$ . The rate law for the first reaction is now given by:

$$v_1 = \frac{k_1 X_o (X_o + 1) (S_I + 1)^2}{(S_I + 1)^2 (X_o + 1)^2 + 80000}.$$

Setting  $X_o = 1$ ,  $k_1 = 100$ ,  $k_2 = 0.14$ , a steady-state concentration of  $S_I$  can be determined to be 66.9. Evaluating the derivative  $\partial d(S_I/dt)/\partial S_I$  at this steady state yields a value of 0.084, which is clearly a positive value. This means that any disturbance to  $S_I$  at this particular steady state will cause  $S_I$  to increase; in other words, this steady state is unstable.

For single variable systems the question of stability reduces to determining the sign of the  $\partial d(S_I/dt)/\partial S_I$  derivative. For larger systems the stability of a system can be determined by looking at all the terms  $\partial d(S_i/dt)/\partial S_i$  which are given collectively by the expression:

$$\frac{d(ds/dt)}{ds} = J, \quad [13]$$

where  $J$  is called the Jacobian matrix containing elements of the form  $\partial d(S_i/dt)/\partial S_i$ . Equation [12] can be generalized to:

$$\frac{d(\delta s)}{dt} = J \delta s.$$

Analysis shows that solutions to the disturbance equations [12] and [13] are sums of exponentials where the exponents of the exponentials are given by the eigenvalues of the Jacobian matrix,  $J$  (53). If the eigenvalues are negative then the exponents decay (stable), whereas if they are positive then the exponents grow (unstable).

Another way to obtain the eigenvalues is to look at the roots (often called the poles in engineering) of the characteristic equation, which can be found in the denominator of the transfer function, Eq. [10]. For stability, the real parts of all the poles of the transfer function should be negative. If any pole is positive, then the system is unstable. The characteristic equation can be written as a polynomial, where the order of the polynomial reflects the size of the model.

$$a_n s^n + a_{n-1} s^{n-1} + \dots + a_1 s + a_0 = 0$$

A test for stability is that all the coefficients of the polynomial must have the same sign if all the poles are to have negative real parts. Also it is necessary for all the coefficients

**Table 13.2**  
**Routh-Hurwitz table**

$a_n$	$a_{n-2}$	$a_{n-4}$	$\cdots$
$a_{n-1}$	$a_{n-3}$	$a_{n-5}$	$\cdots$
$b_1$	$b_2$	$b_3$	$\cdots$
$c_1$	$c_2$	$c_3$	$\cdots$
etc.			

to be nonzero for stability. A technique called the Routh-Hurwitz criterion can be used to determine the stability. This procedure involves the construction of a “Routh Array” shown in **Table 13.2**. The third and fourth rows of the table are computed using the relations:

$$b_1 = \frac{a_{n-1}a_{n-2} - a_n a_{n-3}}{a_{n-1}} \quad b_2 = \frac{a_{n-1}a_{n-4} - a_n a_{n-5}}{a_{n-1}} \text{ etc.}$$

$$c_1 = \frac{b_1 a_{n-3} - b_2 a_{n-1}}{b_1} \quad c_2 = \frac{b_1 a_{n-5} - b_3 a_{n-1}}{b_1} \text{ etc.}$$

Rows to the table are added until a row of zeros is reached. Stability is then determined by the number of sign changes in the **1st** column, which is equal to the number of poles with real parts greater than zero. **Table 13.3** shows the Routh table for the characteristic equation  $s^3 + s^2 - 3s - 1 = 0$  where  $s = i\omega$ . From the **Table 13.3** we see one sign change between the second and the third rows. This tells us that there must be one positive root. Since there is one positive root, the system from which this characteristic equation was derived is unstable.

The advantage of using the Routh-Hurwitz table is that entries in the table will be composed from elasticity coefficients. Thus sign changes (and hence stability) can be traced to particular constraints on the elasticity coefficients. Examples of this will be given in the next section.

**Table 13.3**  
**Routh-Hurwitz table**

1	-3
1	-1
-2	
-1	

### 3.4. Dynamic Motifs

#### 3.4.1. Bistable Systems

The question of stability leads on to the study of systems with non-trivial behaviors. In the previous section a model was considered, which was shown to be unstable. This model was described by the following set of rate equations:

$$v_1 = \frac{k_1 X_o (X_o + 1) (S_1 + 1)^2}{(S_1 + 1)^2 (X_o + 1)^2 + 80000},$$

$$v_2 = k_2 S_1.$$

The network is depicted in **Fig. 13.13** and illustrates a positive feedback loop, that is,  $S_1$  stimulates its own production.

The steady state of this simple model is computed at  $dS_1/dt = v_1 - v_2 = 0$  or  $v_1 = v_2$ . If  $v_1$  and  $v_2$  are plotted against  $S_1$  (**Fig. 13.14**), the points where the curves intersect correspond to the steady states of the system. Inspection of **Fig. 13.14** shows three intersection points.

The steady-state solution that was examined earlier ( $S_1 = 66.9$ ) corresponds to the second intersection point and, as shown, this steady state is unstable. Solutions to the system can be found at

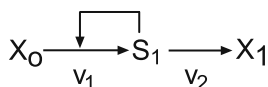


Fig. 13.13. Simple pathway with positive feedback.

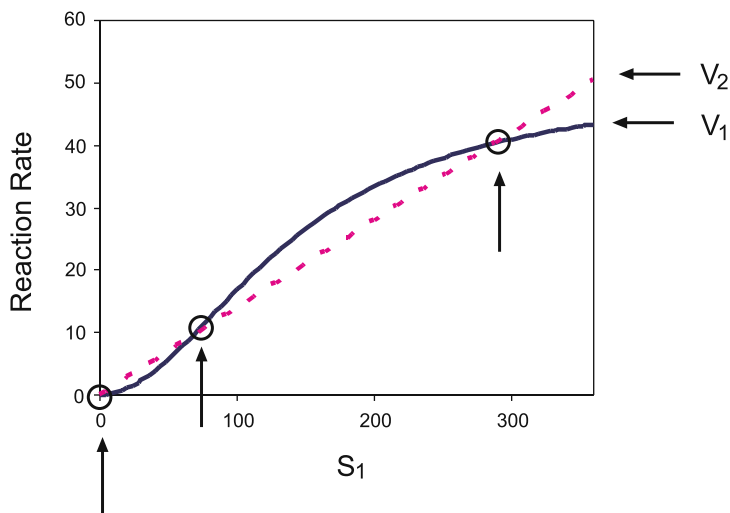


Fig. 13.14. Graph showing  $v_1$  and  $v_2$  plotted against the species concentration,  $S_1$  for the model depicted in **Fig. 13.13**. The intersection points, where  $v_1 = v_2$  are marked with small circles and indicate three possible steady states. Rate equations:  $v_1 = (k_1 X_o (X_o + 1) (S_1 + 1)^2) / ((S_1 + 1)^2 (X_o + 1)^2 + 80000)$ ,  $v_2 = k_2 S_1$ , and parameter values  $X_o = 1$ ,  $k_1 = 100$ ,  $k_2 = 0.14$ . The steady-state solutions correspond to values of  $S_1$  at 0.019, 66.89, and 288.23.

**Table 13.4**  
**Table of steady-state  $S_I$  and corresponding value for the Jacobian element. Negative Jacobian values indicate a stable steady state, positive elements indicate an unstable steady state. The table shows one stable and two unstable steady states**

Steady State $S_I$	Jacobian Element: $(dS_I/dt)/dS_I$
0.019	-0.086
66.89	0.084
288.23	-0.135

values of  $S_I$  at 0.019, 66.89, and 288.23. By substituting these values into the equation for  $dS_I/dt$  we can compute the Jacobian element in each case (Table 13.4).

This system possess three steady states, one unstable and two stable. Such a system is known as a bistable system because it can rest in one of two stable states. One question which arises is what are the conditions for bistability? This can be easily answered using BCT. The unscaled frequency response of  $S_I$  with respect to  $v_I$  can be computed using Eq. [10] to yield:

$$C_{v_I}^{S_I} = \frac{1}{\varepsilon_1^2 - \varepsilon_1^1 + iw}$$

Constructing the Routh-Hurwitz table indicates one sign change, which is determined by the term,  $\varepsilon_1^2 - \varepsilon_1^1$ . Note that  $\varepsilon_1^1$  has a positive value because  $S_I$  activates  $v_I$ . Because the pathway is a linear chain the elasticities can be scaled without changes to the stability terms criterion, thus the pathway is stable if

$$\varepsilon_1^1 > \varepsilon_1^2.$$

If we assume first-order kinetics in the decay step,  $v_2$ , then the scaled elasticity,  $\varepsilon_1^2$  will be equal to unity, hence

$$\varepsilon_1^1 > 1.$$

This result shows that it is only possible to achieve bistability if the elasticity of the positive feedback is greater than one (assuming the consumption step is first order). The only way to achieve this is through some kind of cooperative or multimeric binding, such as dimerization or tetramer formation. The bistability observed in the lac operon is a possible example of this effect (57, 56).

### 3.4.2. Feedback and Oscillatory Systems

The study of oscillatory systems in biochemistry has a long history dating back to at least the 1950s. Until recently, however, there was very little interest in the topic from mainstream molecular biology. In fact, one suspects that the concept of oscillatory behavior in cellular networks was considered more a curiosity, and a rare one at that, than anything serious. With the advent of new measurement technologies, particularly high-quality microscopy, and the ability to monitor specific protein levels using GFP and other fluorescence techniques, a whole new world has opened up to many experimentalists. Of particular note is the recent discovery of oscillatory dynamics in the p53/Mdm2 couple (54, 26) and Nf- $\kappa$ B (41) signaling; thus rather than being a mere curiosity, oscillatory behavior is in fact an important, though largely unexplained, phenomenon in cells.

**Basic Oscillatory Designs.** There are two basic kinds of oscillatory designs, one based on negative feedback and a second based on a combination of negative and positive feedback. Both kinds of oscillatory design have been found in biological systems. An excellent review of these oscillators and specific biological examples can be found in (84, 18). A more technical discussion can be found in (83, 82).

**Negative Feedback Oscillator.** Negative feedback oscillators are the simplest kind to understand and probably one of the first to be studied theoretically (32). Savageau (77) in his book provides a detailed analysis and summary of the properties of feedback oscillators. Figure 8 shows a simple example of a system with a negative feedback loop. We can use BCT to analyze this system by deriving the characteristic equations (the denominator of the frequency response) and constructing a Routh-Hurwitz table. Using this technique it can be easily shown that a pathway with only two intermediates in the feedback loop *cannot* oscillate. In general, a two-variable system with a negative feedback is stable under all parameter regimes. Once a third variable has been added, the situation changes and the pathway shown in **Fig. 13.15**, which has three variables, can admit oscillatory behavior.

A critical factor that determines the onset of oscillations, apart from the number of variables, is the strength of the feedback. Savageau (77) showed that if the substrate elasticities were equal (e.g., all first-order kinetics), then the ratio of the feedback elasticity ( $\epsilon_{inh}$ ) to the output elasticity ( $\epsilon_{sub}, \epsilon_3^4$ ) determined the onset of oscillations (**Table 13.5**). **Table 13.5** shows that as the

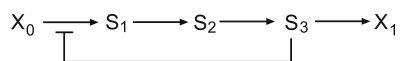


Fig. 13.15. Simple negative feedback model with three variables,  $S_1$ ,  $S_2$ , and  $S_3$ . This network can oscillate.



**Table 13.5**  
**Relationship between the pathway length and the degree of feedback inhibition on the threshold for stability.  $\epsilon_{inh}$  is the elasticity of the feedback inhibition and  $\epsilon_{sub}$  is the elasticity of the distal step with respect to the signal**

Length of pathway	Instability threshold $-\epsilon_{inh}/\epsilon_{sub}$
1	Stable
2	Stable
3	8.0
4	4.0
5	2.9
6	2.4
7	2.1
$\vdots$	$\vdots$
$\infty$	1.0

pathway becomes longer less feedback inhibition is required to destabilize the pathway. This highlights the other factor that contributes to instability, the delay in routing the signal around the network. All feedback oscillators require some device to provide amplification of a signal combined with a suitable time delay so that the signal response can go out of phase. In metabolic pathways, amplification is often provided by a cooperative enzyme while the delay is provided by the intermediate steps in the pathway. In signaling pathways, amplification can be generated by covalent modification cycles. Amplification can also be provided by another means. The criterion for instability is the ratio of the inhibition elasticity to the substrate elasticity. If the output reaction of the pathway is governed by a saturable enzyme, then it is possible to have  $\epsilon_{sub}$  less than unity. This means that it is possible to trade cooperativity at the inhibition site with saturation at the output reaction. The modified Goodwin model of Bliss (7) illustrates the model with no cooperativity at the inhibition site, but with some saturation at the output reaction by using a simple Michaelis-Menten rate law.

A second property uncovered by BCT is that stability is enhanced if the kinetic parameters of the participating reactions are widely separated, that is, a mixture of “fast” and “slow” reactions. The presence of “fast” reactions effectively shortens the pathway, and thus it requires higher feedback strength to destabilize the pathway since the delay is now less.

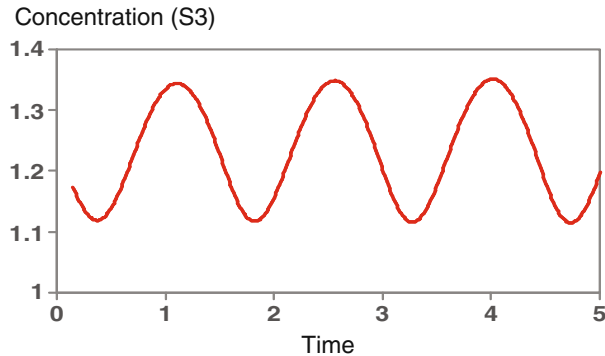


Fig. 13.16. Plot of  $S_3$  versus time for the model shown in Fig. 13.15. Note that the profile of the oscillation is relatively smooth.

One of the characteristics of negative feedback oscillators is that they tend to generate smooth oscillations (Fig. 13.16), and in man-made devices they are often used to generate simple trigonometric functions.

A related oscillator that operates in a similar way to the feedback oscillator is the ring oscillator (See Fig. 13.17). This device is composed of an odd number of signal inverters connected into a closed chain. Instability requires sufficient amplification between each inverter so that the signal strength is maintained. A ring oscillator has been implemented experimentally in *Escherichia coli* (17) where it was termed a repressilator. Ring oscillators with an even number of inverters can be used to form memory units or toggle switches. The even number of units means that the signal latches to either on or off, the final state depending on the initial conditions. Toggle circuits have also been implemented experimentally in *E. coli* (25).

**Relaxation Oscillators.** A favorite oscillator design amongst theorists (58, 63, 22, 23), as well as biological evolution (86, 24, 29, 67, 12), is the relaxation oscillator. This kind of oscillator operates by charging a species concentration that, upon reaching a threshold, changes the state of a bistable switch. When the switch

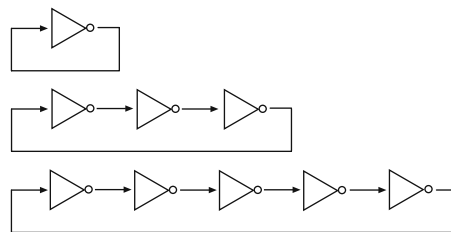


Fig. 13.17. Three ring oscillators, one-stage, three-stage, and five-stage oscillators. All ring oscillators require an odd number of gating elements. Even rings behave as toggle switches.

changes state, it causes the species to discharge. Once the species has discharged, the bistable switch returns to the original state and the sequence begins again. Positive feedback or a two-step ring oscillator forming a toggle switch is used to generate the bistability, and a negative feedback loop provides the signal to switch the bistable switch.

One of the characteristics of a relaxation oscillator is the “spiky” appearance of the oscillations. This is due to the rapid switching of the bistable circuit, which is much faster compared to the operation of the negative feedback. Man-made devices that utilize relaxation oscillators are commonly used to generate saw-tooth signals. **Figure 13.18** illustrates a plot from a hypothetical relaxation oscillator published by Tyson’s group (84).

**Oscillator Classification.** As previously discussed, oscillators fall into two broad categories, feedback oscillators and relaxation oscillators. Within the relaxation oscillation group, some authors (84) have proposed to divide this group into two and possibly three additional subgroups; these include substrate-depletion, activator-inhibitor, and toggle-based relaxation oscillators. The grouping is based on two-variable oscillators and a comparison of the sign patterns in the Jacobian matrix. Although toggle-based relaxation oscillations have the same Jacobian sign pattern as substrate-depletion based oscillations, the bistability is implemented differently.

**Figure 13.19** shows examples of six different oscillators, together with their classification and stylized forms.

Even though each mechanistic form (first column) in **Fig. 13.19** looks different, the stylized forms (second column) fall into one of three types. The stylized forms reflect the structure

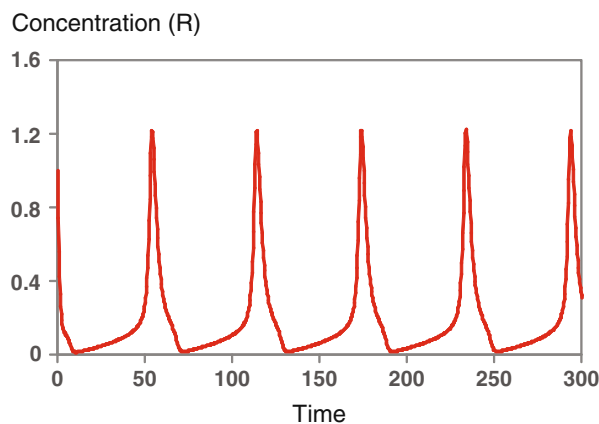


Fig. 13.18. Typical spiky appearance of oscillatory behavior from a relaxation oscillator, from Tyson (84), model 2(c).

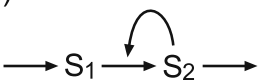
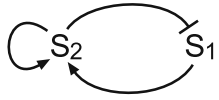
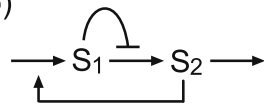
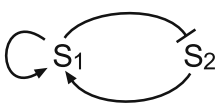
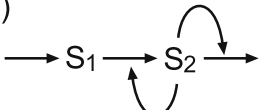
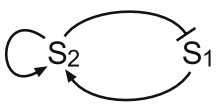
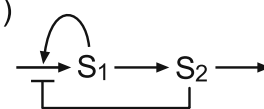
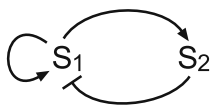
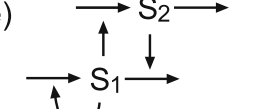
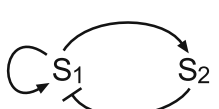
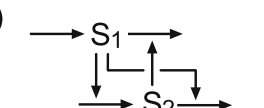
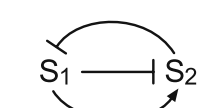
Mechanism	Stylized Form	Type
a) 		<b>SD</b>
b) 		<b>SD</b>
c) 		<b>SD</b>
d) 		<b>AI</b>
e) 		<b>AI</b>
f) 		<b>SD/T</b>

Fig. 13.19. Classification of Relaxation Oscillators into substrate-depletion, activator-inhibitor, and toggle-based. Note that although the mechanistic networks are quite variable, the underlying operation is the same as shown in the stylized column. Type codes: SD = Substrate-Depletion; AI = Activator- Inhibitor; SD/T = Substrate-Depletion/ Toggle. The stylized form is generated by computing the Jacobian matrix for each network. Elements in the Jacobian indicate how each species influences changes in another. Model (a) corresponds to model (c) in **Fig. 13.2** of (84) and model (e) to model (b) in **Fig. 13.2** of (84).

of the Jacobian for each model. Only a limited number of sign patterns in the Jacobian can yield oscillators (39). Using evolutionary algorithms (16, 65), many hundreds of related mechanisms can be generated, see the model repository at [www.sys-bio.org](http://www.sys-bio.org) for a large range of examples. Although many of these evolved oscillators look quite different, each one can be classified in a only a few basic configurations.

---

## 4. Summary

This chapter has focused on describing some of the theory that is available to analyze the dynamics of deterministic/continuous models of biochemical networks. Some areas have been omitted, in particular bifurcation analysis has not been discussed but is probably one of the more important tools at our disposal because it can be used to uncover the different qualitative behavioral regimes a network might possess. Bifurcation analysis would require an entire chapter to describe; however, good starting points include the chapter by Conrad and Tyson (13) and the book by Izhikevich (47).

The most significant area missing from this chapter is undoubtedly a discussion on stochastic modeling (89). As more experimental data becomes available on times series changes in species concentrations, it is becoming abundantly clear that many processes, particularly genetic networks, are noisy. In prokaryotic systems we are often dealing with small numbers of molecules and the stochastic nature of reaction dynamics becomes an important consideration. Unfortunately, there is at present little accessible theory on the analysis of stochastic models, which greatly impedes their utility. In almost all cases, the analysis of stochastic systems relies exclusively on numeric simulation, which means generalizations are difficult to make. Some researches have started to consider the theoretical analysis of stochastic systems (66, 78) and the field is probably one of the more exiting areas to consider in the near future.

---

## 5. Notes



1. A recent and potentially confusing trend has been to use the symbol  $S$  to signify the stoichiometry matrix. The use of the symbol  $N$  has, however, a long tradition in the field, the letter  $N$  being used to represent “number,” indicating stoichiometry. The symbol,  $S$ , is usually reserved for species.
2. There are rare cases when a “conservation” relationship arises out of a non-moiety cycle. This does not affect the mathematics, but only the physical interpretation of the relationship. For example,  $A \rightarrow B + C$ ;  $B + C \rightarrow D$  has the conservation,  $B - C = T$ .
3. Possibly inviting the use of the term, ultra-rate-limiting?

---

## 6. Reading List

The following lists books and articles that cover the material in this chapter in much more depth.

### ***Introductory and Advanced Texts on Systems Analysis***

Fell, D (1996) *Understanding the Control of Metabolism*, Ashgate Publishing, ISBN: 185578047X

Heinrich R, Schuster S (1996) *The Regulation of Cellular Systems*. Chapman and Hall, ISBN: 0412032619

Klipp E, et al. (2005) *Systems Biology in Practice, Concepts, Implementation and Application*. Wiley-VCH Verlag, ISBN: 3527310789

Izhikevich, E. M. (2007) *Dynamical Systems in Neuroscience: The Geometry of Excitability and Bursting*, MIT Press, ISBN: 0262090430

### ***Control Theory***

Ingalls, B. P. (2004) A frequency domain approach to sensitivity analysis of biochemical systems, *Journal of Physical Chemistry B*, 108, 1143–1152

### ***Bistability and Oscillations***

Tyson J, et al. (2003) Sniffers, buzzers, toggles and blinkers: dynamics of regulatory and signaling pathways in the cell. *Current Opinion in Cell Biology*, 15, 221–231

### ***Stochastic Modeling***

Wilkinson D. J. (2006) *Stochastic Modeling for Systems Biology*. Chapman and Hall, ISBN: 1584885408

---

## Acknowledgments

I wish to acknowledge Ravishankar R. Vallabhajosyula for assistance in preparing the simulation data and figures for the gene cascade circuits. This work was supported by a generous grant from the NSF (award number CCF- 0432190).

## References

1. Altan-Bonnet G, Germain RN (2005). Modeling T cell antigen discrimination based on feedback control of digital ERK responses. *PLoS Biol* 3(11):1925–1938.
2. Alves R, Savageau MA (2000). Effect of overall feedback inhibition in unbranched biosynthetic pathways. *Biophys J* 79: 2290–2304.
3. Arkin AP (2000). Signal Processing by Biochemical Reaction Networks. In J. Walleczek (Ed.), *Self-Organized Biological Dynamics and Nonlinear Control*, pp. 112–114. Cambridge University Press.
4. Austin DW, Allen MS, McCollum JM, Dar RD, Wilgus JR, Saylor GS, Samatova NF, et al. (2006). Gene network shaping of

- inherent noise spectra. *Nature* 439(7076): 608–611.
5. Bakker BM, Westerhoff HV, Opperdoes FR, Michels PAM (2000). Metabolic control analysis of glycolysis in trypanosomes as an approach to improve selectivity and effectiveness of drugs. *Mol Biochem Parasitology* 106:1–10.
  6. Blackman FF (1905). Optima and limiting factors. *Ann Botany* 19:281–295.
  7. Bliss RD, Painter PR, Marr AG (1982). Role of feedback inhibition in stabilizing the classical operon. *J Theor Biol* 97(2):177–193.
  8. Blüthgen N, Bruggeman FJ, Legewie S, Herzog H, Westerhoff HV, Kholodenko BN (2006). Effects of sequestration on signal transduction cascades. *FEBS J* 273(5): 895–906.
  9. Burns JA (1971). Studies on Complex Enzyme Systems. Ph. D. thesis, University of Edinburgh. <http://www.cds.caltech.edu/hsauro/Burns/jimBurns.pdf>
  10. Burrell MM, Mooney PJ, Blundy M, Carter D, Wilson F, Green J, Blundy KS, et al. (1994). Genetic manipulation of 6-phosphofruktokinase in potato tubers. *Planta* 194:95–101.
  11. Burton AC (1936). The basis of the principle of the master reaction in biology. *J Cell Comp Physiol* 9(1):1–14.
  12. Chen KC, Calzone L, Csikasz-Nagy A, Cross FR, Novak B, Tyson JJ (2004). Integrative analysis of cell cycle control in budding yeast. *Mol Biol Cell* 15(8): 3841–3862.
  13. Conrad ED, Tyson JJ (2006). Modeling Molecular Interaction Networks with Non-linear Ordinary Differential Equations. In J. S. Zoltan Szallasi and V. Periwal (Eds.), *System Modeling in Cellular Biology From Concepts to Nuts and Bolts*, Chapter 6, pp. 97–123. MIT Press.
  14. Cornish-Bowden A, Hofmeyr JHS (2002). The Role of Stoichiometric Analysis in Studies of Metabolism: An Example *J Theor Biol* 216:179–191.
  15. Cox C, McCollum J, Austin D, Allen M, Dar R, Simpson M (2006). Frequency domain analysis of noise in simple gene circuits. *Chaos* 16(2):26102–26102.
  16. Deckard A, Sauro HM (2004). Preliminary studies on the in silico evolution of biochemical networks. *Chembiochem* 5:1423–31.
  17. Elowitz MB, Leibler S (2000). A synthetic oscillatory network of transcriptional regulators. *Nature* 403:335–338.
  18. Fall CP, Marland ES, Wagner JM, Tyson JJ (2002). *Computational Cell Biology*. Springer-Verlag.
  19. Fell DA, Sauro HM (1985a). Metabolic control analysis: additional relationships between elasticities and control coefficients. *Eur J Biochem* 148:555–561.
  20. Fell DA, Sauro HM (1985b) Substrate cycles: do they really cause amplification? *Biochem Soc Trans* 13:762–763.
  21. Fell DA, Sauro HM (1990). Metabolic control analysis: the effects of high enzyme concentrations. *Eur J Biochem* 192: 183–187.
  22. Field RJ, Koros E, Noyes RM (1972). Oscillations in chemical systems, Part 2. Thorough analysis of temporal oscillations in the bromate-cerium-malonic acid system. *J Am Chem Soc* 94:8649–8664.
  23. Field RJ, Noyes RM (1974). Oscillations in chemical systems. IV. Limit cycle behavior in a model of a real chemical reaction. *J Chem Phys* 60(5):1877–1884.
  24. FitzHugh R (1955). Mathematical models of threshold phenomena in the nerve membrane. *Bull Math Biophys* 17:257–278.
  25. Gardner TS, Cantor CR, Collins JJ (2000). Construction of a genetic toggle switch in *Escherichia coli*. *Nature* 403:339–342.
  26. Geva-Zatorsky N, Rosenfeld N, Itzkovitz S, Milo R, Sigal A, Dekel E, Yarnitzky T, et al. (2006). Oscillations and variability in the p53 system. *Mol Syst Biol* 2:2006–2006.
  27. Gillespie DT (1976). A general method for numerically simulating the stochastic time evolution of coupled chemical reactions. *J Comp Phys* 22:403–434.
  28. Gillespie DT Exact stochastic simulation of coupled chemical reactions. *J Phys Chem* 81:2340–2361.
  29. Goldbeter A (1997). *Biochemical Oscillations and Cellular Rhythms: The Molecular Bases of Periodic and Chaotic Behaviour*. Cambridge University Press;
  30. Goldbeter A, Koshland DE (1981). An amplified sensitivity arising from covalent modification in biological systems. *Proc Natl Acad Sci* 78:6840–6844.
  31. Goldbeter A, Koshland DE (1984). Ultra-sensitivity in biochemical systems controlled by covalent modification. Interplay between zero-order and multistep effects. *J Biol Chem* 259:14441–14447.
  32. Goodwin B (1965). Oscillatory behaviour in enzymatic control processes. *Adv Enzyme Regul* 3:425–438.

33. Hearon JZ (1952). Rate behavior of metabolic reactions. *Physiol Rev* 32:499–523.
34. Heinisch J (1986). Isolation and characterisation of the two structural genes coding for phosphofruktokinase in yeast. *Mol Gen Genet* 202:75–82.
35. Heinrich R, Rapoport TA (1974a). A linear steady state treatment of enzymatic chains. Critique of the crossover theorem and a general procedure to identify interaction sites with an effector. *Eur J Biochem* 42:97–105.
36. Heinrich R, Rapoport TA (1974b). A linear steady-state treatment of enzymatic chains; general properties, control and effector strength. *Eur J Biochem* 42:89–95.
37. Heinrich R, Schuster S (1996). *The Regulation of Cellular Systems*. Chapman and Hall.
38. Higgins J (1965). Dynamics and control in cellular systems. In B. Chance, R. W. Estabrook, and J. R. Williamson (Eds.), *Control of Energy Metabolism*, pp. 13–46. Academic Press.
39. Higgins J (1967). The Theory of Oscillating Reactions. *Ind Eng Chem* 59(5):18–62.
40. Higgins JJ (1959). Ph. D. thesis: A theoretical study of the kinetic properties of sequential enzyme reactions, Univ. Pennsylvania.
41. Hoffmann A, Levchenko A, Scott ML, Baltimore D (2002). The Ikappa B-NF-kappa B signaling module: temporal control and selective gene activation. *Science* 298:1241–1245.
42. Hofmeyr JHS (1986). Steady state modelling of metabolic pathways: a guide for the prospective simulator. *Comp Appl Biosci* 2:5–11.
43. Hofmeyr JHS (2001). Metabolic Control Analysis in a Nutshell. In *Proceedings of the Second International Conference on Systems Biology*. Caltech.
44. Hofmeyr JS, Cornish-Bowden A (2000). Regulating the cellular economy of supply and demand. *FEBS Lett* 476(1–2):47–51.
45. Ingalls BP (2004). A frequency domain approach to sensitivity analysis of biochemical systems. *J Phys Chem B* 108:1143–1152.
46. Ingolia NT (2004). Topology and robustness in the Drosophila segment polarity network. *PLoS Biol* 2(6):805–815.
47. Izhikevich EM (2007). *Dynamical systems in neuroscience: the geometry of excitability and bursting*. MIT Press.
48. Kacser H (1983). The control of enzyme systems in vivo: elasticity of the steady state. *Biochem Soc Trans* 11:35–40.
49. Kacser H, Burns JA (1973). The Control of Flux. In D. D. Davies (Ed.), *Rate Control of Biological Processes*, Volume 27 of *Symp Soc Exp Biol*, pp. 65–104. Cambridge University Press.
50. Kacser H, Burns JA (1981). The molecular basis of dominance. *Genetics* 97(3–4): 639–666.
51. Kaern M, Weiss R (2006). Synthetic Gene Regulatory Systems. In J. S. Zoltan Szallasi and V. Periwal (Eds.), *System Modeling in Cellular Biology From Concepts to Nuts and Bolts*, Chapter 13, pp. 269–298. MIT Press.
52. Kholodenko BN (2006). Cell-signalling dynamics in time and space. *Nat Rev Mol Cell Biol* 7(3):165–176.
53. Klipp E, Herwig R, Kowald A, Wierling C, Lehrach H (2005). *Systems Biology in Practice*. Wiley-VCH Verlag.
54. Lahav G, Rosenfeld N, Sigal A, Geva-Zatorsky N, Levine AJ, Elowitz MB, Alon U (2004). Dynamics of the p53-Mdm2 feedback loop in individual cells. *Nat Gen* 36(2):147–150.
55. LaPorte DC, Walsh K, Koshland DE (1984). The branch point effect. Ultrasensitivity and subsensitivity to metabolic control. *J Biol Chem* 259(22):14068–14075.
56. Laurent M, Kellershohn N (1999). Multistability: a major means of differentiation and evolution in biological systems. *TIBS* 24:418–422.
57. Levandoski MM, Tsodikov OV, Frank DE, Melcher SE, Saecker RM, Record MT, Jr (1996). Cooperative and anticooperative effects in binding of the first and second plasmid Osym operators to a LacI tetramer: evidence for contributions of non-operator DNA binding by wrapping and looping. *J Mol Biol* 260(5):698–717.
58. Lotka AJ (1920). Undamped oscillations derived from the law of mass action. *J Am Chem Soc* 42:1595–1599.
59. Mangan S, Alon U Structure and function of the feed-forward loop network motif. *Proc Natl Acad Sci USA* 100(21):11980–11985.
60. Markevich NI, Hoek JB, Kholodenko BN (2004). Signaling switches and bistability arising from multisite phosphorylation in protein kinase cascades. *J Cell Biol* 164:353–359.
61. Mettetal JT, Muzzey D, Pedraza JM, Ozbudak EM, van Oudenaarden A (2006). Predicting stochastic gene expression dynamics in single cells. *Proc Natl Acad Sci USA* 103(19):7304–7309.



62. Morales MF (1921). A note on limiting reactions and temperature coefficients. *J Cell Comp Physiol* 30:303–313.
63. Nicolis G (1971). Stability and dissipative structures in open systems far from equilibrium. *Adv Chem Phys* 19:209–324.
64. Ortega F, Garcés JL, Mas F, Kholodenko BN, Cascante M (2006). Bistability from double phosphorylation in signal transduction. *FEBS J* 273(17):3915–3926.
65. Paladugu S, Chickarmane V, Deckard A, Frumkin J, McCormack M, Sauro H (2006). In silico evolution of functional modules in biochemical networks. *IEE Proc-Systems Biol* 153:223–235.
66. Paulsson J, Elf J (2006). Stochastic Modeling of Intracellular Kinetics. In J. S. Zoltan Szallasi and V. Periwal (Eds.), *System Modeling in Cellular Biology From Concepts to Nuts and Bolts*, Chapter 8, pp. 149–175. MIT Press.
67. Pomerening JR, Sontag ED, Ferrell JE (2003). Building a cell cycle oscillator: hysteresis and bistability in the activation of Cdc2. *Nat Cell Biol* 5(4):346–351.
68. Rao CV, Sauro HM, Arkin AP (2004). Putting the ‘Control’ in Metabolic Control Analysis. 7th International Symposium on Dynamics and Control of Process Systems, DYCOPS, 7.
69. Reder C (1988). Metabolic control theory: a structural approach. *J Theor Biol* 135:175–201.
70. Reder C, Mazat JP (1988). Aspects géométriques de la théorie du contrôle du métabolisme in: Le contrôle du métabolisme. Master’s thesis, Bordeaux.
71. Reich JG, Selkov EE (1981). Energy metabolism of the cell. Academic Press.
72. Sauro HM (1994). Moiety-conserved cycles and metabolic control analysis: problems in sequestration and metabolic channelling. *BioSystems* 33:15–28.
73. Sauro HM, Ingalls B (2004). Conservation analysis in biochemical networks: computational issues for software writers. *Biophys Chem* 109(1):1–15.
74. Sauro HM, Kholodenko BN (2004). Quantitative analysis of signaling networks. *Prog Biophys Mol Biol* 86:5–43.
75. Savageau MA (1972). The behaviour of intact biochemical control systems. *Curr Topics Cell Reg* 6:63–130.
76. Savageau MA (1974). Optimal design of feedback control by inhibition: steady-state considerations. *J Mol Evol* 4:139–156.
77. Savageau MA (1976). Biochemical systems analysis: a study of function and design in molecular biology. Addison-Wesley.
78. Scott M, Ingalls B, Kærn M (2006). Estimations of intrinsic and extrinsic noise in models of nonlinear genetic networks. *Chaos* 16(2):26107–26107.
79. Small JR, Fell DA (1990). Covalent modification and metabolic control analysis: modification to the theorems and their application to metabolic systems containing covalently-modified enzymes. *Eur J Biochem* 191:405–411.
80. Stucki JW (1978). Stability analysis of biochemical systems – a practical guide. *Prog Biophys Mol Biol* 33:99–187.
81. Thomas S, Fell DA (1994). MetaCon – a program for the algebraic evaluation of control coefficients of arbitrary metabolic networks. In H. V. Westerhoff (Ed.), *Biothermokinetics*, pp. 225–229. Intercept Ltd.
82. Tyson J, Othmer HG (1978). The dynamics of feedback control circuits in biochemical pathways. In R. Rosen and F. M. Snell (Eds.), *Progress in Theoretical Biology*, 5:1–62.
83. Tyson JJ (1975). Classification of instabilities in chemical reaction systems. *J Chem Phys* 62:1010–1015.
84. Tyson JJ, Chen KC, Novak B (2003). Sniffers, buzzers, toggles and blinkers: dynamics of regulatory and signaling pathways in the cell. *Curr Opin Cell Biol* 15:221–231.
85. Vallabhajosyula RR, Chickarmane V, Sauro HM (2006). Conservation analysis of large biochemical networks. *Bioinformatics* 22(3):346–353.
86. van der Pol B, van der Mark J (1928). The heartbeat considered as a relaxation oscillation, and an electrical model of the heart. *Philos Mag Suppl* 6:763–775.
87. Voit E, Neves AR, Santos H (2006). The intricate side of systems biology. *Proc Natl Acad Sci USA* 103(25):9452–9457.
88. Westerhoff HV, Chen YD (1984). How do enzyme activities control metabolite concentrations? *Eur J Biochem* 142:425–430.
89. Wilkinson DJ (2006). Stochastic Modelling for Systems Biology. Chapman and Hall.